





Article

Coastal Pine-Oak Glacial Refugia in the Mediterranean Basin: A Biogeographic Approach Based on Charcoal Analysis and Spatial Modelling

Gaetano Di Pasquale ¹, Antonio Saracino ¹, Luciano Bosso ^{1,*}, Danilo Russo ¹,
Adriana Moroni ², Giuliano Bonanomi ¹ and Emilia Allevato ^{1,*}

¹ Department of Agricultural Sciences, University of Naples Federico II, via Università 100, 80055 Portici, Italy; gaetano.dipasquale@unina.it (G.D.P.); antonio.saracino@unina.it (A.S.); danilo.russo@unina.it (D.R.); giuliano.bonanomi@unina.it (G.B.)

² Department of Physical, Earth and Environmental Sciences, Prehistory and Anthropology Research Unit, University of Siena, via Laterina 8, 53100 Siena, Italy; adriana.moroni@unisi.it

* Correspondence: luciano.bosso@unina.it (L.B.); eallevat@unina.it (E.A.)

Received: 12 May 2020; Accepted: 10 June 2020; Published: 12 June 2020



Abstract: During the glacial episodes of the Quaternary, European forests were restricted to small favourable spots, namely refugia, acting as biodiversity reservoirs. The Iberian, Italian and Balkan peninsulas have been considered as the main glacial refugia of trees in Europe. In this study, we estimate the composition of the last glacial forest in a coastal cave of the Cilento area (SW Italy) in seven time frames, spanning from the last Pleniglacial to the Late Glacial. Charcoal analyses were performed in seven archaeological layers. Furthermore, a paleoclimate modelling (Maxent) approach was used to complement the taxonomic identification of charcoal fragments to estimate the past potential distribution of tree species in Europe. Our results showed that the mesothermophilous forest survived in this region in the core of the Mediterranean basin during the Last Glacial Period (LGP, since ~36 ka cal BP), indicating that this area played an important role as a reservoir of woodland biodiversity. Here, *Quercus pubescens* was the most abundant component, followed by a wide variety of deciduous trees and *Pinus nigra*. Charcoal data also pointed at the crucial role of this coastal area, acting as a reservoir for warm temperate trees of genera *Tilia*, *Carpinus* and *Sambucus*, in LGP, in the Mediterranean region. Our modelling results showed that *P. nigra* might be the main candidate as a “*Pinus sylvestris* type” in the study site in the Last Glacial Maximum (LGM). Furthermore, we found that *P. nigra* might coexist with *Q. pubescens* in several European territories both currently and in the LGM. All models showed high levels of predictive performances. Our results highlight the advantage of combining different approaches such as charcoal analysis and ecological niche models to explore biogeographic questions about past and current forest distribution, with important implications to inform today’s forest management and conservation.

Keywords: Charcoal; Ecological Niche Model; Forest History; Last Glacial Maximum; Maxent; Paleoecology; *Pinus nigra*; *Pinus mugoluncinata*; *Pinus sylvestris*; *Quercus pubescens*

1. Introduction

Present-day Mediterranean vegetation is the result of the interaction of several factors and processes including past glaciation, location of refuge areas, biogeographic barriers and from the middle Holocene onwards, also anthropogenic influence [1–3].

During the Pleistocene, the advance and retreat of the ice sheets, due to climatic oscillations, had severe impacts on the distributions of many animal and plant species, which were able to survive only in suitable unglaciated habitat available during at least part of the ice ages [4].

These climate refugia have a major role in explaining modern patterns of biodiversity and species distribution [5].

As a general rule, the Iberian, Italian and Balkan peninsulas, which remained relatively ice-free and probably supported relict soils [6], have been identified as the main glacial tree refugia areas in Europe [7,8].

The location of refuge areas and the patterns of the northward spread of deciduous species during the Pleistocene–Holocene transition has been approached with many different methodologies, such as phylogeography, fossil records and Ecological Niche Models (ENMs) [5]. These synergistic approaches are being increasingly used in a combination, but to date, the studies carried out lack geographical precision in seeking to pinpoint the location of such refugia [5,9–13]. In this context, fossil records provide the best evidence for the presence of a species within a slice of both space and time. Among them, if on the one hand, palynology has long been the main technique used for paleobotanical studies [5], on the other hand, charcoal analysis has been less widely applied [10].

Charcoal analysis (anthracology) is especially suitable in the Mediterranean region where conservative environments for pollen, limited to acid and poorly aerated peat bogs and lakes, are scarce [10,14]. Although charcoals are not deposited in a continuous way, unlike pollen grains, they can provide a higher spatial resolution than pollen, because charcoals are not carried by the wind over long distances. Thus, charcoal data provide information at a local spatial scale since they testify for the local presence of the tree taxon from which they originate [10]. Unfortunately, the accuracy of paleoecological analysis, both for charcoal and pollen, is affected by inherent limitations due to the fact that taxonomic identification is not always reliable to the species level [15].

In the context of paleobiology, ENMs are being increasingly used to complement fossil and genetic evidence in biogeographical or paleontological reconstructions [16–19]. Such tools may provide an in-depth understanding of temporal changes in species distributions and their interactions with past environments. The increasing development and availability of paleoclimate data [20,21] have improved both temporal range and resolution of ENM applications, which may add effectively to fossil and genetic analysis to clarify past distribution patterns of plants, animals or biological communities [19,22,23].

The Mediterranean basin is an outstanding biodiversity hotspot with a prominent reservoir role for plant richness [7]. In this context, human cave settlements represent an exceptional paleoenvironmental archive for fine-scale biogeographic reconstruction [24].

In this study, we estimate the extent of the last glacial forest in a coastal cave of the Cilento area (SW Italy). Scarce pollen data, available for the last glacial cycle in southern Italy, revealed a peculiar difference in taxa composition, mostly related to geographical and topographic features (i.e., latitude and elevation) of the pollen catchment area. In this region of Italy, pollen data from a marine area provided information on the last 28,000 years of vegetation dynamics [25]. This data covering both mountain and coastal belts suggested that during the last glacial cycle open landscapes dominated by steppe elements coexisted with *Pinus* and forest of mesophilous taxa such *Abies* and deciduous broadleaved *Quercus* [25]. So far, the potential distribution of *Pinus* in Europe including the Italian territory during LGM has been scarcely explored [3,26]. The two above-mentioned modelling studies showed contrasting results on the presence of *P. sylvestris* in southern Italy. In fact, Cheddaddi et al. [3] showed that *P. sylvestris* potentially occurred in central Italy while Svenning et al. [26] reported *P. sylvestris* for several areas in southern Italy. A small wild population of *Pinus nigra* currently occurs near our study site (Mts. Picentini, Vallone della Caccia) [27] while the wild population of *P. sylvestris* are restricted to northern Italy [28]. Here, we used a combination of charcoal analysis and spatial modelling to test the hypothesis that charcoals found in our study site might actually belong to *P. nigra*.

As species identification by charcoal analysis alone is problematic due to the absence of specific diagnostic key features, this hypothesis was explored using an ENM for all the species belonging to the *P. sylvestris* type found in the study site through charcoal analyses and developing models for the LGM, assessing past potential environmental suitability for the different species [15].

2. Materials and Methods

2.1. Study Area

The Cilento region (Figure 1) presents several cave human settlements embracing a wide period from the Paleolithic up to the Bronze Age [29]. Serratura Cave (hereafter abbreviated as SC, Figure 1, Figure S1), located in Camerota Bay (40°00' N; 15°22' E), belongs to the geological unit of Mt Bulgheria (1,225 m a.s.l.). The SC is located ca. 20 m inland from the coastline, at 2 m a.s.l. and has an area of ~70 m². The cave preserves long-term Late Pleistocene–Holocene stratigraphic successions, which have a prominent position in the prehistoric framework of the southern Italian mainland [30,31].

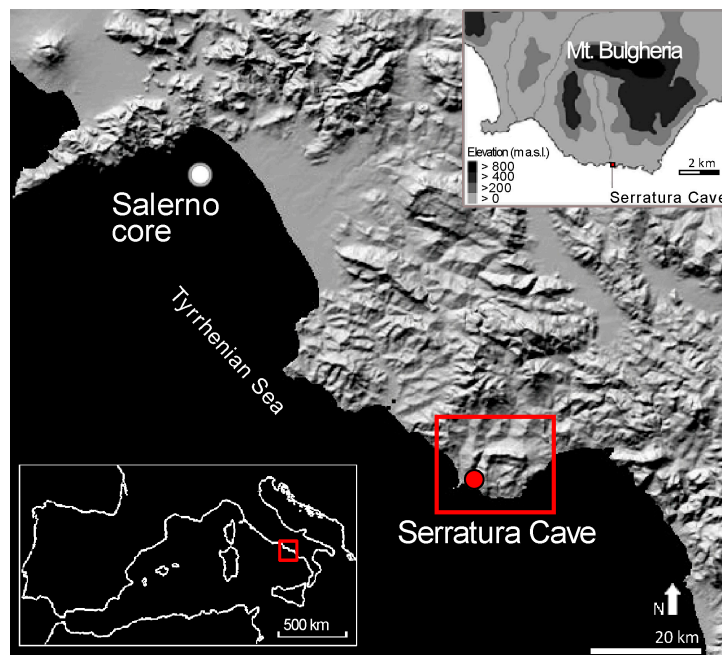


Figure 1. Geographical position of the Serratura Cave on the coast of Cilento (southern Italy, 40°00' N; 15°22' E).

The current climate of Camerota Bay is subhumid thermo-Mediterranean. Temperatures never fall below 0 °C and the mean annual temperature is 14.8 °C (Capo Palinuro, 185 m a.s.l.). Precipitation has a mean annual value of 762 mm (referred to years 1958–1999) and is irregularly distributed throughout the year, with only 4.7% falling during the summer (July and August).

In the coastal sector, Mediterranean maquis dominates vegetation, with *Pistacia lentiscus*, *Phillyrea latifolia*, *Juniperus phoenicea*, *Euphorbia dendroides*, *Calicotome villosa*, *Spartium junceum* *Myrtus communis* and several *Cistus* species. In xeric sites degraded by recurrent wildfires, the tussock grass *Ampelodesmos mauritanicus* is the dominant species. Scattered large, old *Quercus pubescens* trees occur along the coast, whereas further inland, the vegetation is dominated by *Q. ilex*, accompanied by *P. latifolia* and *M. communis* and some deciduous species such as *Q. pubescens*, *Fraxinus ornus* and *Ostrya carpinifolia*. In the submontane and montane sector small *Q. pubescens* woods together with *Castanea sativa* and *Q. cerris* woods are present. From 1000 m a.s.l. up to the treeline, large *Fagus sylvatica* forests are found [32].

2.2. Charcoal Analysis

Sediment samples were collected during the archaeological excavations [30,31] and then sieved in situ by water through a sieving column. All charcoal fragments ranging between 2 and 4 mm mesh sizes were sorted under a dissection microscope and then analysed using a reflected light microscope (100X–1000X). Taxonomic identification relied on the reference collection of plant and wood anatomy,

and wood anatomy atlases [33–37]. Relevant specific literature was used to reach the species level identification in the taxonomic group of deciduous *Quercus* [36].

We analysed charcoal from the Late Pleistocene layers, whose stratigraphy, the corresponding ^{14}C dating and cultural facies, are shown in Table 1.

Table 1. Age and cultural facies of Serratura Cave layers (SW Italy). Conventional ^{14}C ages were calibrated using the OxCal v. 4.3 program (Bronk Ramsey, 2009) and the IntCal3 calibration curve data (Reimer et al., 2013). Calibrated calendar years before present (cal BP) expressed as either a two-sigma probability age range and a median probability age.

Layer	Cultural Facies	^{14}C Dating (yr BP)	Calibrated Ages $\pm 2\sigma$ (cal yr BP)	Median cal yr BP	Chronostratigraphy
8E	Final Epigravettian	11,490 \pm 160	13,708–13,057	13,332	Late Glacial
8F		11,460 \pm 80	13,455–13,135	13,305	Late Glacial
8G		12,060 \pm 90	14,150–13,730	13,915	Late Glacial
9	Evolved	13,100 \pm 120	16,063–15,302	15,702	Late Glacial
10C	Epigravettian	15,700 \pm 110	19,234–18,724	18,953	Pleniglacial
11	Gravettian	24,380 \pm 1530	32,574–25,925	28,874	Pleniglacial
12		29,020 \pm 2650	43,290–28,645	34,269	Pleniglacial

Sampling layers were selected to collect only scattered charcoal (sensu Chabal) [38], because these fragments, resulting from long-term burning activities, can be considered representative of local vegetation and thus suitable for paleoecological studies [10,39–42]. A minimum of 200 charcoal fragments were examined for each layer except Layer 11, where the available number of fragments was limited to 100. Charcoal frequencies were calculated for all layers. While quantitative data were not shown for Layer 12, a fireplace where charcoals probably represent the remnants of a single burning event of collected wood [38].

2.3. Ecological Niche Model

2.3.1. Training and Projection Area

As training and projection areas we considered the European and North Africa territories comprised between latitudes 30° N–70° N and longitudes 15° W–35° E.

2.3.2. Data Collection

To collect occurrence records of the taxa of interest identified through charcoal analysis, we used several sources as: (1) public access databases, including the European forest genetic resources programme (<http://www.euforgen.org>) and the European Information System on Forest Genetic Resources (<http://portal.eufgis.org/>) and (2) shapefiles obtained by Caudullo et al. [43]. We screened all the records in ArcGis (version 10.2.2; <http://www.esri.com/software/arcgis>) for spatial autocorrelation using average nearest neighbour analyses and Moran's I measure of spatial autocorrelation to remove spatially correlated data points and guarantee independence [44,45]. After spatial autocorrelation analysis of our dataset, to generate ENMs we used only fully independent presence records falling within the native range as described by Caudullo et al. [43] (Supplementary Materials, Figures S2–S5).

2.3.3. Environmental Variables

To build the ENMs for our taxa, we started from a set of 19 bioclimatic variables obtained from the WorldClim database vers. 2.0. (www.worldclim.org/current) [21]. We downloaded the bioclimatic variables in a consistent format (ESRI grid file) and resolution (2.5 min resolution, approximately

5 km grid cell sizes at the equator). Then, we converted all the bioclimatic variables in ASCII files and generated a Pearson's correlation matrix with SDMtoolbox (version 2.2) [46] in ArcGis (version 10.2.2; <http://www.esri.com/software/arcgis>). From the matrix, we selected only the variables for which $r < 0.70$ [47–49] in order to remove any variables that could be highly correlated with one another before developing the models. Pearson's correlation matrix led to a final set of 5 climatic variables: temperature seasonality (%), mean temperature of the wettest quarter (°C), mean temperature of the driest quarter (°C), precipitation of driest month (mm) and precipitation of coldest quarter (mm). We used these variables to carry out ENMs in current and in Last Glacial Maximum (LGM) scenarios.

2.3.4. Maxent Models

We built ENMs using the maximum entropy modelling approach, Maxent ver. 3.4.1 (http://biodiversityinformatics.amnh.org/open_source/maxent/) [50]. This algorithm usually provides an excellent predictive approach compared with other modelling methods and is especially suited to deal with scarce presence-only data [51–54]. Since this technique relies on a generative rather than a discriminative approach, it performs well when the amount of training data is limited. Because our study area was small, we trained models using data from the entire European territory to account for a more comprehensive niche representation.

We carried out an ENM for each of the taxa identified in the cave by charcoal analysis using three steps: (1) we ran current models using presence records and the bioclimatic variables selected as described above; (2) we carried out paleoclimate models projecting current distribution in the LGM scenarios; and (3) we again ran paleoclimate models projecting current distribution in the LGM scenarios, but only for some taxa selected in Step 2. Unlike the previous model, here, we added the potential distribution map of the best-represented taxon in the study area using it as an “bioclimatic variables”.

From the Maxent's setting panel, we selected the following options: random seed; remove duplicate presence records; write plot data; regularisation multiplier (fixed at 1) [50]; 1000 maximum iterations, 10,000 background points, cloglog format (this output appears to be most appropriate for estimating the probability of presence) [54,55]; and, finally, we used a 20-replicate effect with cross-validation run type. This run type makes it possible to replicate n-sample sets removing one locality at a time [22,56]. We fixed to 1 the default regularisation value as this is based on the different performances recorded across a range of taxonomic groups [57]. The remaining model values were set to default values [22,58].

For each species, the average final map had a cloglog output format with suitability values from 0 (unsuitable habitat) to 1 (suitable habitat). The 10th percentile (the value above which the model classifies correctly 90% of the training locations) was selected as the threshold value for defining the species' presence. This is a conservative value commonly applied to ecological niche modelling studies, particularly those relying on datasets collected over a long time by different observers and methods [22,56,58,59]. We used this threshold to reclassify our model into binary presence/absence maps.

We generated the paleoclimate models using the same climatic variables above described. These models were trained with all occurrences collected, and projected to Europe in the LGM (23,000–18,000 years BP). We developed the paleoclimate models using the most used LGM scenarios: CCSM4 [19,60,61]. Projecting ENMs to regions other than those where models were calibrated, or to past or future times is a common approach to make inferences such as forecasting the spreading of alien organisms, providing paleo-reconstructions or predicting distributional patterns in future epochs [62,63]. In order to project to new area models calibrated elsewhere, whether in the current epoch or in the LGM, variables in the projection area must meet a condition of environmental similarity to the environmental data used for training the model. Therefore, we first ascertained that this condition occurred by inspecting the Multivariate Environmental Similarity Surfaces (MESS) generated by Maxent [64,65].

2.3.5. Model Validation

We tested the predictive performance of models using the receiver operating characteristics, for which we analysed the Area Under Curve (AUC) [66], and the minimum difference between training and testing AUC data (AUC_{diff}) [67]. These model evaluation statistics range between 0 and 1. Excellent model performances are expressed respectively by AUC values close to 1 and AUC_{diff} close to 0.

2.3.6. Resolving Taxonomic Ambiguity by Means of ENM

In this study, several charcoal fragments were identified as “*Pinus sylvestris* type” (see Results). Materials classified as *Pinus sylvestris* type might correspond to *Pinus sylvestris*, *Pinus nigra* and *Pinus mugo/uncinata*, but species identification by charcoal analysis is somewhat problematic due to the absence of specific diagnostic key features.

Therefore, we first generated ENMs for the three species mentioned above, along with *Q. pubescens*, because this was the most common taxon identified at species level at the site (see Results). In a second step, we used the *Q. pubescens* potential distribution as an environmental layer for the above-mentioned *Pinus* models, assuming that the species found in the same charcoal assemblage should have similar ecological requirements since, these prehistoric communities collected wood fuel in the immediate surroundings of human settlements [41].

3. Results

3.1. Charcoal Analysis

We identified 1677 charcoal fragments and established the occurrence of 12 taxa (Figure 2; Supplementary Materials, Figure S6).

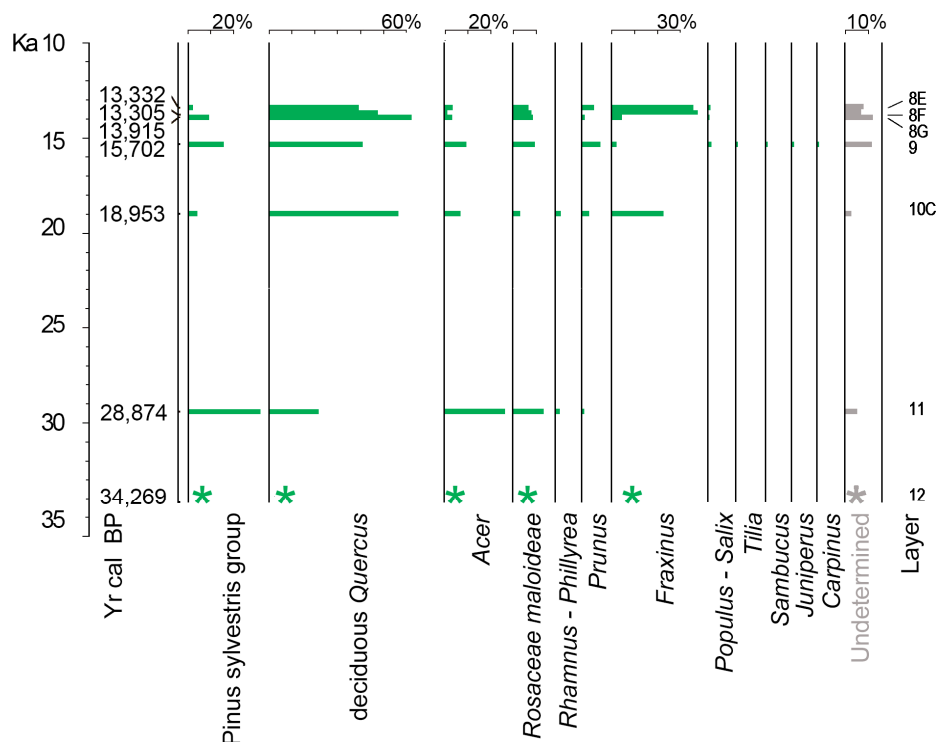


Figure 2. Charcoal percentages of the Serratura Cave plotted against age (y cal BP). Calibrated age BP are expressed as the median probability age.

Quercus deciduous type, namely *Q. pubescens*, was the best-represented taxon in almost all investigated layers, ranging from 61% (Layer 8) to 21% (Layer 11, Figure 2). Although deciduous

Quercus can be hard to distinguish at the species level, the porous ring with only one to two rows of large vessels in the earlywood and their diameter never exceeding 250 μm , allowed us to identify *Q. pubescens*. *Fraxinus ornus-oxycarpa* was represented in all the SC layers, apart from Layer 11. Based on the comparison of autecological features, both species are conceivable since *F. ornus* could belong to the mesoxerophilous forest community while *F. oxycarpa* could be restricted to lowland and riparian areas forming the mesohygrophilous azonal forest together with *Populus* and/or *Salix* attested in Layers 9, 8F and 8E. *Acer* (excluded *A. pseudoplatanus* and *A. platanoides*) was present in all samples; the maximum value (28%) is attested in Layer 11 and the minimum (4%) in Layer 8E. *Tilia*, *Carpinus* and *Sambucus* were attested with low values (0.5–1.3%) especially in Layer 9. Coniferous wood was represented by *Pinus sylvestris* type and *Juniperus*. *Pinus sylvestris* type was present in all layers, with its maximum value in the Layer 11 (30%), while *Juniperus* was attested by a few wood charcoals in Layer 9. Rosaceae Maloideae were always attested in all the charcoal assemblages, their value ranging from 3% (Layer 10) to 13% (Layer 11). *Prunus* was present in SC Layers 11, 10C, 8G and 8E with a maximum value of 7.9%.

3.2. Ecological Niche Models of *Pinus* spp. and *Q. pubescens*

3.2.1. Current Models

The analysis of single variable contribution showed that temperature seasonality, mean temperature of wettest quarter and precipitation of driest month were the main factors influencing the model performance for all the tree species. We found that the accumulated contribution of these three variables was 88%, 83%, 93% and 81% for *P. mugo/uncinata*, *P. nigra*, *P. sylvestris* and *Q. pubescens*, respectively. The current model predicted a high probability of potential distribution of *P. mugo/uncinata* especially in the Alps and other European mountain areas, whereas *P. nigra* was more likely to occur in central and southern Europe and in western Asia, *P. sylvestris* in central and northern Europe and in western Asia and *Q. pubescens* in central and southern Europe (Figures 3 and 4).

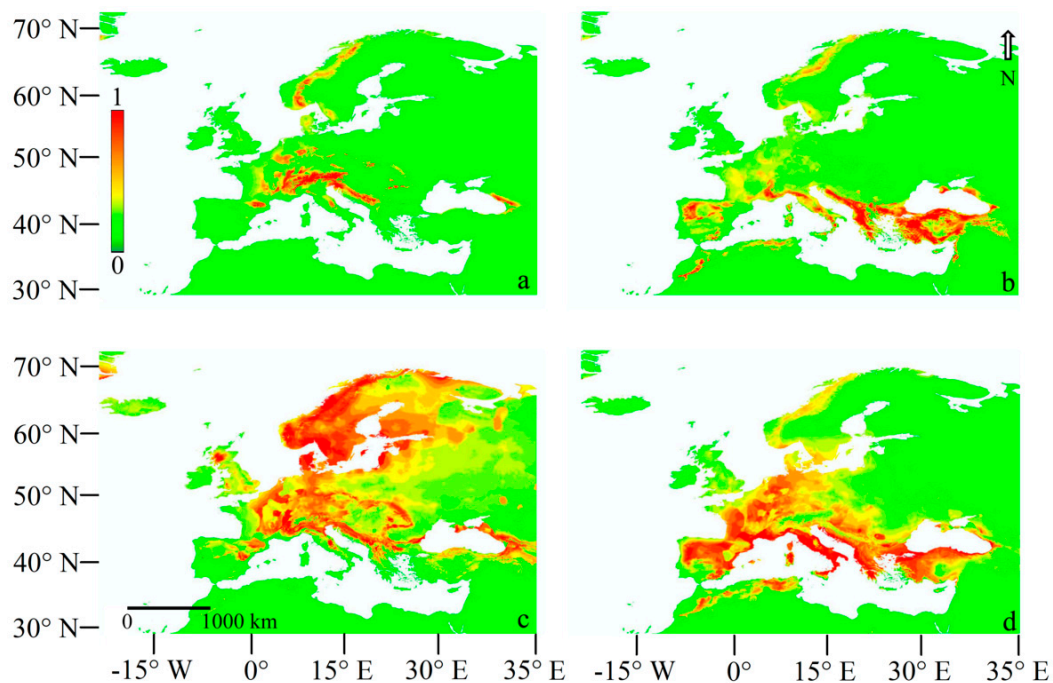


Figure 3. Ecological Niche Models for *P. mugo/uncinata* (a), *P. nigra* (b), *P. sylvestris* (c) and *Q. pubescens* (d) using current scenario. Scales show the probability of presence ranging from 0 to 1.

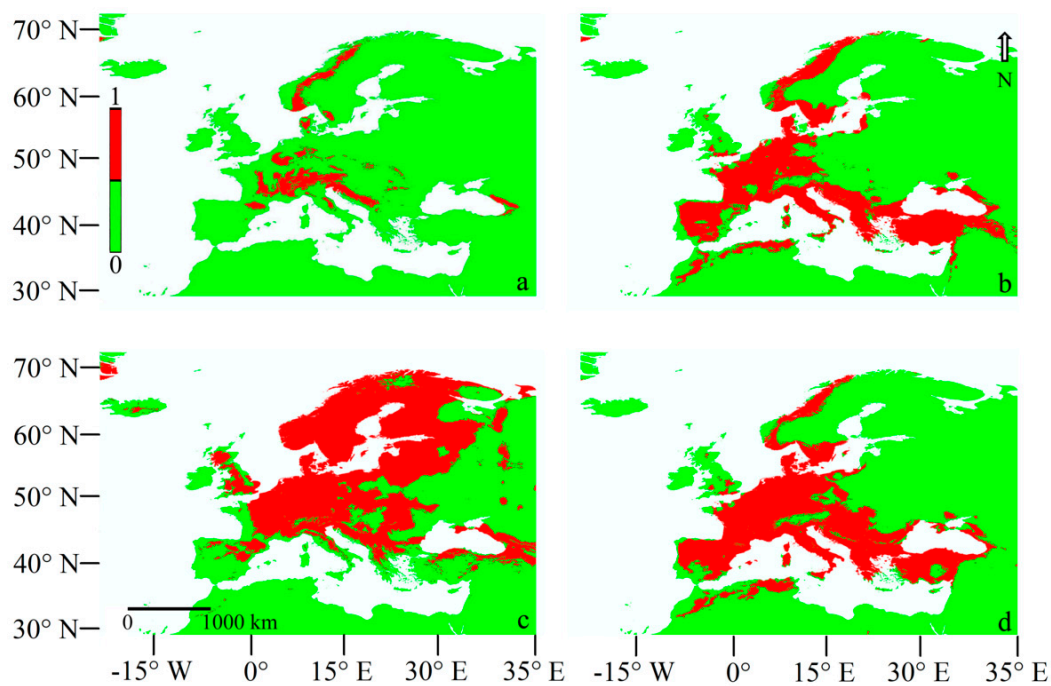


Figure 4. Ecological Niche Models for *P. mugo/uncinata* (a), *P. nigra* (b), *P. sylvestris* (c) and *Q. pubescens* (d) using the current scenario. Binary map shows: 0 = unsuitable habitat; 1 = suitable habitat.

3.2.2. Last Glacial Maximum Projection Models

The LGM model predicted a high probability of potential distribution of *P. mugo/uncinata* especially in central and western Europe, whereas *P. nigra* was more likely to occur in southern Europe and in western Asia, *P. sylvestris* in western, central and northern Europe and in western Asia and *Q. pubescens* in southern Europe (Figures 5 and 6).

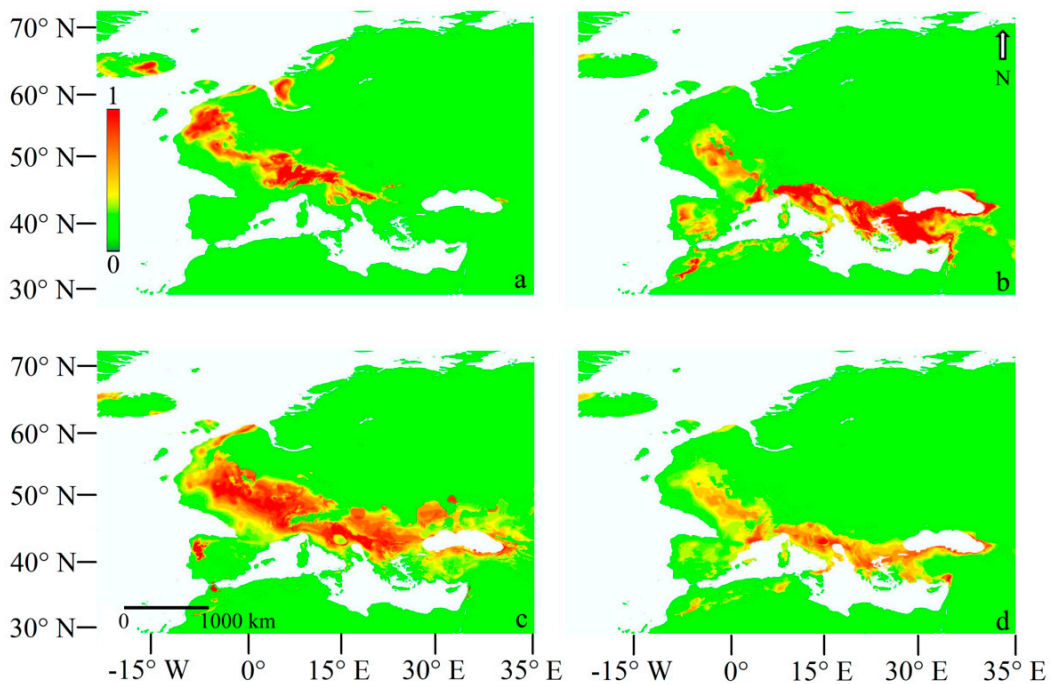


Figure 5. Ecological Niche Models for *P. mugo/uncinata* (a), *P. nigra* (b), *P. sylvestris* (c) and *Q. pubescens* (d) using the Last Glacial Maximum scenario. Scales show the probability of presence ranging from 0 to 1.

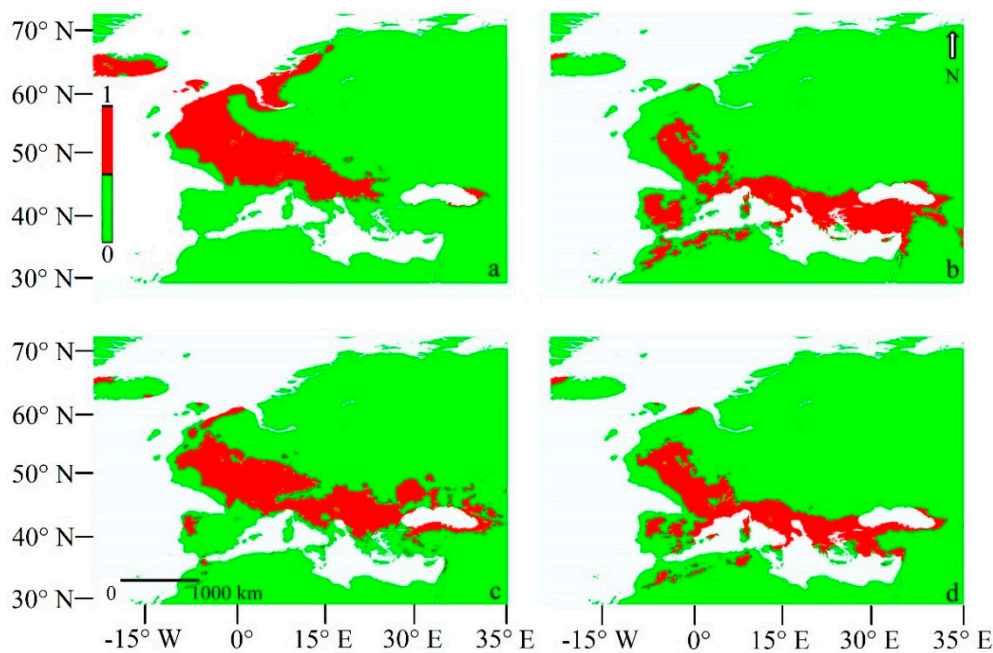


Figure 6. Ecological Niche Models for *P. mugo/uncinata* (a), *P. nigra* (b), *P. sylvestris* (c) and *Q. pubescens* (d) using the Last Glacial Maximum scenario. Binary map shows: 0 = unsuitable habitat; 1 = suitable habitat.

The MESS analysis showed negative values of environmental similarities for *P. mugo/uncinata*, *P. nigra*, *P. sylvestris* and *Q. pubescens* only in the northeast area of the map in comparison to the training area (Supplementary Materials, Figures S7–S10), whereas positive values were obtained for central and southern areas (Supplementary Materials, Figures S7–S10). Maxent models for *P. mugo/uncinata*, *P. nigra*, *P. sylvestris* and *Q. pubescens* showed AUC of 0.968 ± 0.032 , 0.908 ± 0.082 , 0.816 ± 0.076 and 0.859 ± 0.073 , respectively. AUC_{diff} mean and standard deviation's values for all the Maxent models were <0.1 .

3.2.3. LGM Projection Models Adding the *Q. pubescens* Distribution

The analysis of single variable contribution showed that temperature seasonality, mean temperature of wettest quarter and precipitation of driest month were the main factors influencing the model performance for *P. mugo/uncinata* and *P. sylvestris*. We found that the accumulated contribution of these three variables was 80% and 92% for *P. mugo/uncinata* and *P. sylvestris*, respectively. Instead, the potential distribution of *Q. pubescens* was the main layer influencing the model performance of *P. nigra* with a contribution of ca. 70% versus 30% and barely 8% of influence in *P. sylvestris* and *P. mugo/uncinata* model, respectively. The MESS analysis and the potential distributions of *P. mugo/uncinata*, *P. nigra* and *P. sylvestris* were not affected by the presence of the variable *Q. pubescens*' potential distribution. In fact, both the trend of MESS results and of the potential distributions of the three *Pinus* were similar to those obtained from the previous first models.

Maxent models for *P. mugo/uncinata*, *P. nigra* and *P. sylvestris* showed an AUC of 0.958 ± 0.028 , 0.912 ± 0.079 and 0.845 ± 0.066 , respectively. AUC_{diff} mean and standard deviation's values for all the Maxent models were <0.1 .

4. Discussion

4.1. *Pinus Type Sylvestris*: Ecological Niche Models and Ecological Considerations

Our ENMs showed considerable performances in estimating the current and past distributions of *P. mugo/uncinata*, *P. nigra*, *P. sylvestris* and *Q. pubescens* in Europe, as also shown by model validation.

AUC values such as the ones that we obtained (>0.8) are among the highest reported for published models (e.g., [44,53]) and documented a high predictive power of habitat suitability [68]. Our study was further supported by AUC_{diff} values (e.g., [47]).

In agreement with Caudullo et al. [43], our current models for Europe matched well the observed distribution of *P. mugo/uncinata*, *P. nigra*, *P. sylvestris*, while, with regard to *Q. pubescens*, the models identified a larger area than that shown in Caudullo et al. [43], in our case comprising the whole of the Iberian Peninsula. *P. mugo/uncinata* occurs in the mountains of Central and Eastern Europe, but is especially abundant in the subalpine belt of the Eastern Alps and the Carpathians [42]. Disjunct ranges occur in the lower mountains of the Jura and the Vosges, and at high altitudes in the Mediterranean and Balkan Mountains, such as the Apennines, the Albanian Alps and the Rila-Pirin-Rhodopes in Bulgaria [43]. Indeed, in Italy, *P. mugo/uncinata* belongs strictly to the subalpine belt, occurring above the forest treeline in the Alps and locally in the northern-central Apennines [69]. *P. sylvestris* ranges from Scotland, Ireland and Portugal in the west, east to eastern Siberia, south to the Caucasus Mountains and north to the Arctic Circle in Scandinavia [7] while, in Italy, it spreads to the Alps and occurs as a relic in the northern Apennines [69]. The *P. nigra* group is a widely distributed Mediterranean mountain conifer with a discontinuous range extending from North Africa (35° N), through the northern Mediterranean, eastwards to the Black sea, finally in the western Mediterranean on the islands of Corsica and Sicily (both as *P. nigra* subsp. *laricio*). In southern Italy, *P. nigra* forests are today confined to a few relic carbonatic rocky mountains where they form open vegetation on the steep slopes between the grasslands and the broadleaved forest [27]. *Q. pubescens* ranges from the Atlantic coast of France to the shores of the Mediterranean Sea, and across peninsular Italy, the Balkan Peninsula and the Aegean regions, to the coasts of the Black Sea and most of Anatolia. Although our models showed that *Q. pubescens* might potentially occur in the entire Iberian Peninsula, the western extreme of its geographic range, to the best of our knowledge, pubescent oak lives only in northern Spain [43]. This is not surprising since ENMs do not take into account biotic interactions such as competition, nor they may include historical factors which might play a role in influencing actual distribution [70]. In Italy, according to our models, this species occurs on almost the entire territory [69].

The substantial matching between our models and the maps shown in Caudullo et al. [43] represent an encouraging piece of evidence supporting the reliability of the maps of past predicted distribution of *P. mugo/uncinata*, *P. nigra*, *P. sylvestris* and *Q. pubescens* in Italy. The past dynamics of *Pinus* species, and consequently their paleobiogeography, are poorly documented because pollen and charcoal studies do not allow confident species identification. Regarding the Iberian Peninsula, paleoecologists mention the occurrence of *P. sylvestris* and *P. nigra* probably because both species are currently present in the mountain areas of this region [71]. An integrated paleobotanic, genetic and modelling approach pointed at the existence of western Europe of potential glacial refugia of *P. sylvestris* up to 40° N [3]. The few preceding modelling studies of *P. sylvestris* past potential distribution (e.g., [3,16,26]) showed contrasting results. Habitat suitability modelling of the boreal *P. sylvestris* [3] indicated a potentially wide LGM range in southern Central Europe and eastwards, but those models covered a smaller area than the one we predicted and indicated that potential glacial refugia of *P. sylvestris* were located between ca. 40° N and 50° N with a patchy geographical distribution. Svenning et al.'s Maxent models [26], instead, showed a potential distribution that extended over southern Italy more than ours. Such discrepancies may be due to the different modelling approaches or climatic variables used in such studies. Based on our models, we predicted that in our study area and more generally over southern Italy, *P. nigra* represents the most likely candidate. In fact, neither past potential distribution of *P. mugo/uncinata* nor that of *P. sylvestris* reached our study region in the LGM.

Besides, based on the assumption that the ecological requirements of *P. nigra* match closely those of *Q. pubescens*, we found that the potential distribution of the latter species contributed only 30% to the potential occurrence of *P. sylvestris* vs. 70% to that of *P. nigra*, further corroborating our findings.

Two subspecies of *P. nigra* are described for Italy [72], the subsp. *nigra* and the subsp. *laricio* (*P. nigra* and *P. laricio* sensu Pignatti [69]), respectively. The former has several scattered populations

from 200 to 1500 m a.s.l. in the northeastern Alps, while small patches grow on calcareous slopes in the central-southern Apennines between 100 and 1350 m a.s.l. [73]. *P. n. laricio* mostly grows on siliceous soils, in the Sila region (Calabria) between 900 and 1600 m a.s.l. and in Mt. Etna (Sicily) between 1200 and 2000 m a.s.l. [69,73]. In our area, the dominance of carbonatic substrate is a strong argument against the occurrence of *P. nigra* subsp. *laricio* which is strictly linked to siliceous substrates.

Today, *P. nigra* forests are extremely rare in southern Italy. It is an early successional species, and pure self-replacing forests are constrained to few mountainous Mediterranean areas where they can be considered an edaphic climax limited to thin soils. More often this species is part of precursor or transitional associations towards deciduous broadleaved forests. However, *P. nigra* communities are still present, with a very small population, just ca. 80 km north to our study site on a subcoastal Mesozoic limestone ridge (Mts. Picentini, Vallone della Caccia), where these stands are part of the xerophilic open vegetation that occurs on the steep slopes as transitional vegetation between the grasslands and the broadleaved forest vegetation [27]. The *Pinus nigra*-*Q. pubescens* association which characterises the Pleniglacial could indicate at the local scale a warm-cool bioclimate sensu Finlayson et al. [74].

4.2. Vegetation Cover of the Pleniglacial

The vegetation, inferred at three temporally distinct episodes, was located close to the coastal caves, in a wide coastal plain including currently submerged sectors. Indeed, between 30 and 19 ka cal BP the coastline would have been about 8 km away from the present one, due to sea level lowering [75].

In both the oldest layers, namely at ~36 ka cal BP and at ~29 ka cal BP vegetation cover at the site can be envisaged as woodland with coexisting *P. nigra* and deciduous mesoxerophilous trees with *Q. pubescens* and *Acer*, which summed together, account for the 50% of the charcoal assemblage. Interestingly, the youngest layer falls in the cold arid period detected in the Salerno Gulf, ~80 km to the north, spanning between 34 and 27 ka cal BP [76]. In this phase, despite the occurrence of the lowest values of annual temperatures [TANN (7° C)], July temperatures [TJUL (20° C)] and annual precipitation [PANN (400 mm year⁻¹)], it seems that in Camerota Bay the amount of precipitation may still support the development of forest vegetation.

At ~19 ka cal BP, vegetation is still dominated by *Q. pubescens* and *Fraxinus* (up to ~70%), but the number of pine charcoals appears significantly reduced. The age of this layer falls in the LGM, as defined by EPILOG [77] during which cold arid conditions are inferred for the whole Mediterranean area [78]. However, at the regional scale, this period coincides with the end of a relatively warm-humid phase (25.5 to 18.5 ka cal BP [76]) also recorded at Monticchio (~100 km NE) between 25 and 20 ka BP [79] which might explain the high amount of *Q. pubescens* and *Fraxinus*. This may well have disadvantaged the light-demanding *P. nigra* [80] which probably was restricted to the rocky slopes with thin soils. Overall, during the Pleniglacial, our data suggest a stable forest cover with temporal phases of dominance variation between *Pinus* and deciduous trees.

The presence of a continuous forest cover in the Camerota Bay is also confirmed by the presence of woodland mammals such as Gliridae, Muridae and *Clethrionomys* [81,82], while species related to open and steep slope environments are very rare [83]. The broad diversity of micromammal assemblages throughout the Pleniglacial indicates the contemporaneous presence of probably both forested and open environments that periodically expanded and retreated, offering habitats for many taxa [81].

In a wider spatiotemporal perspective, our data are consistent with the pollen record from the Gulf of Salerno [25], where arboreal pollen values are almost always over 30% and deciduous oaks were stable at around 10% (*Pinus* excluded) during the entire Last Glacial Period (LGP). Our data, combined with the evidence of the almost treeless grass-dominated landscape inland and the much higher elevation sites of the Italian peninsula [79,84,85], suggest that most of the arboreal pollen content of these pollen spectra should be ascribed to the coastal sector.

The only Italian pollen record showing a vegetation cover comparable to that shown by our data concerns the north Tyrrhenian coast where until ~28 ka cal BP deciduous *Quercus* and *Pinus* with *Abies alba* combined to form a dense forest [86].

Roughly at the same latitude as Camerota Bay, the southern Adriatic coast of Italy, at a direct distance of ~200 km, at ~28.5 ka cal BP (24,410 ± 320 BP), was characterised by evergreen vegetation with *P. halepensis*, *Juniperus* and *Pistacia* [87], testifying warmer and drier conditions in this eastern coastal sector.

Such evidence highlights the remarkable vegetation cover heterogeneity in the Italian peninsula both in terms of latitude and longitude during the late Pleistocene, probably due also to a west-east precipitation gradient due to the longitudinal split by the Apennines which intercept and block westerly humid air masses. Our data also highlight the role of local topography on climate: indeed, here, the proximity of the Bulgheria massif probably played a preeminent role in trapping the clouds of the western weather systems spreading from the Tyrrhenian sea.

Interestingly, a good match with our data has also been found along the west Atlantic coast of Portugal, where wood remains of *Pinus nigra/sylvestris*, deciduous *Quercus* and *Fraxinus* dated between 34 to 20 ka BP suggest a very similar forest cover [88]; also, in this case, it seems that oceanic humid air masses played a major role.

In our reconstruction of the forest structure, the spatial position of the pioneer and shade-intolerant black pine with low-density canopy overtops a matrix of mesothermophilous winter deciduous broadleaved species. This structure is today detectable in *P. nigra* and *P. leucodermis* relict forests of southern Italy. Indeed, Rauh's canopy architecture model of these pines exhibits in the mature-old ontogenetic stage a tabular canopy with the green crown restricted to the upper third of the stem and large branches similar to the stem [89–91]. This feature favours direct light transmission and thus permits the establishment of relative shade-tolerating trees, grasses and shrubs. We should also speculate on the engineering capability of the pine canopies, which positively modifies the microclimate by affecting near-ground temperatures, soil moisture and wind speed. In such circumstances, these trees, by acting as nurse plants, should facilitate both establishment and survival of the broadleaved tree species.

In Europe, today, mixed *P. nigra* deciduous forests can be seen in the Eastern Alps where it occurs between 200 to 1200 m a.s.l. together with *O. carpiniifolia* and *F. ornus*; in southern Bulgaria *P. nigra* grows at low altitudes mixed with *Q. frainetto* and *Q. pubescens*; further, in southern France mixed forests with *Q. pubescens* and *P. nigra* can also be found [92].

Forest vegetation probably that is very similar to the one suggested by our charcoal assemblage is the Beynam forest, located in the Kuyrukçu Mountains, not far from Ankara, in central Turkey [93]. According to Emberger's climate classification, this region is characterised by semi-arid and very cold Mediterranean climate [94]. Thus, the summer temperatures and the coldness of winter are the main factors characterising the climate. This forest is entirely surrounded by steppe and it is dominated by *P. nigra* subsp. *pallasiana*, *Q. pubescens* and *Juniperus oxycedrus*. Interestingly, in this region holly oak is not a tree but a shrub, and characterises the lowest layer of the forest cover. This present landscape seems to be the most similar vegetation to the Pleniglacial cover in Camerota Bay.

4.3. Vegetation Cover of the Late Glacial

During the last glacial-interglacial transition (Late Glacial sensu Orombelli et al. [95]), *Q. pubescens* is still the dominant species, accompanied by other deciduous taxa; *P. nigra* is also still present. It should be pointed out that around ~16 ka cal BP new temperate warm taxa such as *Tilia*, *Carpinus* and *Sambucus* appear. This evidence can be interpreted as a clear consequence of the temperature rise and increased soil moisture supply following the beginning of deglaciation. The expansion of *Tilia* recorded in several Late Glacial pollen sequences of southern [96] and central Italy [86,97–101] might reflect an early expansion of that tree from nearby refugia. This hypothesis agrees with the previous ones of shelter

areas for *Tilia* in the lower *thalwegs* of the Mediterranean coastal rivers [102]. The presence of *Populus* agrees with the riparian forest evidence inferred by paleo-shell analysis carried out in the cave [103].

In Layers 8G, 8F, 8E (13.9–13.4 ka cal BP) *P. nigra* declines when *Fraxinus* increases. At this time, in the Gulf of Salerno, a rapid climatic change, culminating at 13.8 ka cal BP, marks the Bølling-Allerød chronozone characterised by the increase in atmospheric temperatures, especially the summer values [TJUL (24 °C)], and precipitation [PANN 900 mm] [76]. Additionally, stable isotopes of land snail shells from the SC layers dated to 14–13.4 ka cal BP suggest moisture conditions quite similar to those of the present day must have occurred. These climatic conditions could have reduced the competitive advantage of *P. nigra* over the broadleaf species, especially with respect to pioneer species such as *F. ornus*. In this respect, it is interesting to note that, in medium and high belt wooded landscapes of Iberian Peninsula, cryophilous pines, that were the main species during the Late Glacial, declined in favour of broadleaved species following Holocene climate amelioration [104].

To sum up, our data suggest that the Cilento coast acted as a refugium for temperate deciduous tree species and *P. nigra*, confirming the coastal environment as a potential reservoir of biodiversity [105,106] and contrasting with the mid-altitude theory based on the assumption that precipitation in this region would have been higher than on the plains [1,2,96,107–109].

Our results remark the usefulness of combining different approaches to explore biogeographic questions about past and current forest distribution—a fundamental step to informing forest management and conservation.

5. Conclusions

Our results give a very clear picture of bioclimatic conditions in the surroundings of the Camerota caves during the LGM and as late as the Lateglacial. They indicate that the climatic conditions were always able to sustain forest cover. The data show the presence of mesothermophilous forest during the LGM (from ~36 ka cal BP), proving that this area played an important role as a reservoir of woodland biodiversity in which *Q. pubescens* was the most abundant component, followed by a wide variety of deciduous trees and mountain pines, most likely *P. nigra*. ENM projections provided a useful complement to our paleoecological studies, refining charcoal evidence and offering a less subjective picture of past geographic distributions of *Pinus* species in the LGM. Ours is the first study that, by using paleoclimate model and charcoal analysis, suggests the potential presence of a glacial refugium of *P. nigra* on the Tyrrhenian coastal sector of southern Italy, confirming our initial hypothesis. Finally, this work provides punctual evidence of the crucial role of coastal areas as reservoirs for temperate tree taxa in the Mediterranean basin.

Supplementary Materials: The following are available online at <http://www.mdpi.com/1999-4907/11/6/673/s1>, Figure S1: Serratura Cave entrance; Figure S2: Presence records of *P. mugo/uncinata* after spatial autocorrelation analysis; Figure S3: Presence records of *P. nigra* after spatial autocorrelation analysis; Figure S4: Presence records of *P. sylvestris* after spatial autocorrelation analysis; Figure S5: Presence records of *Q. pubescens* after spatial autocorrelation analysis; Figure S6: Microscopic anatomical features of main identified taxa; Figure S7: Multivariate Environmental Similarity Surfaces (MESS) maps for *P. mugo/uncinata* obtained with CCSM4 models for LGM scenarios; Figure S8: Multivariate Environmental Similarity Surfaces (MESS) maps for *P. nigra* obtained with CCSM4 models for LGM scenarios; Figure S9: Multivariate Environmental Similarity Surfaces (MESS) maps for *P. sylvestris* obtained with CCSM4 models for LGM scenarios; Figure S10: Multivariate Environmental Similarity Surfaces (MESS) maps for *Q. pubescens* obtained with CCSM4 models for LGM scenarios.

Author Contributions: Conceptualisation, G.D.P., E.A., A.S., L.B. and A.M.; methodology, G.D.P., E.A. and L.B.; software, L.B.; charcoal analysis, G.D.P. and E.A.; formal analysis, E.A., L.B.; resources, G.D.P. and A.M.; data curation, E.A.; writing—original draft preparation E.A., G.D.P. and L.B.; writing—review and editing, D.R., A.S. and G.B.; supervision, E.A.; visualisation, E.A. and L.B.; funding acquisition, A.S. All authors have read and agreed to the published version of the manuscript.

Funding: This research received no external funding. The APC was funded by PSR CAMPANIA 2014–2020 misura 16.5.1—Azioni congiunte per la mitigazione dei cambiamenti climatici e l’adattamento ad essi e per pratiche ambientali in corso Progetto: Cilento: suolo paesaggio e biodiversità (CiSPaB) CUP B12D18000090007, granted to A.S.

Acknowledgments: We are grateful to Federica Furlanetto and Mario Marziano for the technical support given in the early phases of the work.

Conflicts of Interest: The authors declare no conflicts of interest.

References

- Bennett, K.D.; Tzedakis, P.C.; Willis, K.J. Quaternary refugia of north European trees. *J. Biogeogr.* **1991**, *18*, 103–115. [[CrossRef](#)]
- Brewer, S.; Cheddadi, R.; De Beaulieu, J.L.; Reille, M. The spread of deciduous *Quercus* throughout Europe since the last glacial period. *Ecol. Manag.* **2002**, *156*, 27–48. [[CrossRef](#)]
- Cheddadi, R.; Vendramin, G.G.; Litt, T.; François, L.; Kageyama, M.; Lorentz, S.; Laurent, J.-M.; De Beaulieu, J.-L.; Sadori, L.; Jost, A.; et al. Imprints of glacial refugia in the modern genetic diversity of *Pinus sylvestris*. *Glob. Ecol. Biogeogr.* **2006**, *15*, 271–282. [[CrossRef](#)]
- Hewitt, G. The genetic legacy of the Quaternary ice ages. *Nature* **2000**, *405*, 907–913. [[CrossRef](#)]
- Gavin, D.G.; Fitzpatrick, M.C.; Gugger, P.F.; Heath, K.D.; Rodríguez-Sánchez, F.; Dobrowski, S.Z.; Hampe, A.; Sheng Hu, F.; Ashcroft, M.B.; Bartlein, P.J.; et al. Climate refugia: Joint inference from fossil records, species distribution models and phylogeography. *New Phytol.* **2014**, *204*, 37–54. [[CrossRef](#)] [[PubMed](#)]
- Gibbard, P.; Ehlers, J. Extent and chronology of Quaternary glaciation. *Episodes* **2008**, *31*, 211–218.
- Quézel, P.; Médail, F. *Ecologie et Biogéographie des Forêts du Bassin Méditerranéen*; Elsevier: Paris, France, 2003.
- Gómez, A.; Lunt, D.H. Refugia within refugia: Patterns of phylogeographic concordance in the Iberian Peninsula. In *Phylogeography of Southern European Refugia*; Weiss, S., Ferrand, N., Eds.; Springer: Dordrecht, The Netherlands, 2007; pp. 155–188.
- Willis, K.J.; Whittaker, R.J. The refugial debate. *Science* **2000**, *287*, 1406–1407. [[CrossRef](#)]
- Figueiral, I.; Mosbrugger, V. A review of charcoal analysis as a tool for assessing Quaternary and Tertiary environments: Achievements and limits. *Paleogeogr. Paleoclimatol. Paleocol.* **2000**, *164*, 397–407. [[CrossRef](#)]
- Taberlet, P.; Cheddadi, R. Quaternary refugia and persistence of biodiversity. *Science* **2002**, *297*, 2009–2010. [[CrossRef](#)]
- Waltari, E.; Hijmans, R.J.; Peterson, A.T.; Nyári, Á.S.; Perkins, S.L.; Guralnick, R.P. Locating Pleistocene refugia: Comparing phylogeographic and ecological niche model predictions. *PLoS ONE* **2007**, *2*, e563. [[CrossRef](#)]
- Médail, F.; Diadema, K. Glacial refugia influence plant diversity patterns in the Mediterranean Basin. *J. Biogeogr.* **2009**, *36*, 1333–1345. [[CrossRef](#)]
- Renfrew, C.; Bahn, P.G. *Archaeology: Theories, Methods and Practice*; Thames and Hudson: London, UK, 2016.
- Scheel-Ybert, R. Anthracology: Charcoal Analysis. In *Encyclopedia of Global Archaeology*; Smith, C., Ed.; Springer: New York, NY, USA, 2018; pp. 1–11.
- Svenning, J.-C.; Fløjgaard, C.; Marske, K.A.; Nógues-Bravo, D.; Normand, S. Applications of species distribution modeling to paleobiology. *Quat. Sci. Rev.* **2011**, *30*, 2930–2947. [[CrossRef](#)]
- Eduardo, A.A.; Martinez, P.A.; Gouveia, S.F.; da Silva Santos, F.; de Aragao, W.S.; Morales-Barbero, J.; Kerber, L.; Liparini, A. Extending the paleontology–biogeography reciprocity with ENMs: Exploring models and data in reducing fossil taxonomic uncertainty. *PLoS ONE* **2018**, *13*, e0194725. [[CrossRef](#)]
- Jurestovsky, D.; Joyner, T.A. Applications of species distribution modeling for paleontological fossil detection: Late Pleistocene models of Saiga (Artiodactyla: Bovidae, *Saiga tatarica*). *Paleobiodivers. Paleoenviron.* **2018**, *98*, 277–285. [[CrossRef](#)]
- Ribeiro, M.M.; Roque, N.; Ribeiro, S.; Gaviños, C.; Castanheira, I.; Quinta-Nova, L.; Albuquerque, T.; Gerassis, S. Bioclimatic modeling in the Last Glacial Maximum, Mid-Holocene and facing future climatic changes in the strawberry tree (*Arbutus unedo* L.). *PLoS ONE* **2019**, *14*, e0210062. [[CrossRef](#)]
- Hijmans, R.J.; Cameron, S.E.; Parra, J.L.; Jones, P.G.; Jarvis, A. Very high resolution interpolated climate surfaces for global land areas. *Int. J. Climatol. J. R. Meteorol. Soc.* **2005**, *25*, 1965–1978. [[CrossRef](#)]
- Fick, S.E.; Hijmans, R.J. WorldClim 2: New 1-km spatial resolution climate surfaces for global land areas. *Int. J. Climatol.* **2017**, *37*, 4302–4315. [[CrossRef](#)]
- Tang, C.Q.; Dong, Y.-F.; Herrando-Moraira, S.; Matsui, T.; Ohashi, H.; He, L.-Y.; Nakao, K.; Tanaka, N.; Tomita, M.; Li, X.-S. Potential effects of climate change on geographic distribution of the Tertiary relict tree species *Davidia involucrata* in China. *Sci. Rep.* **2017**, *7*, 43822. [[CrossRef](#)]

23. Zhou, W.; Ji, X.; Obata, S.; Pais, A.; Dong, Y.; Peet, R.; Xiang, Q.-Y.J. Resolving relationships and phylogeographic history of the *Nyssa sylvatica* complex using data from RAD-seq and species distribution modeling. *Mol. Phylogenetics Evol.* **2018**, *126*, 1–16. [[CrossRef](#)]
24. Bailey, G.; Carrion, J.S.; Fa, D.A.; Finlayson, C.; Finlayson, G.; Rodriguez-Vidal, J. The coastal shelf of the Mediterranean and beyond: Corridor and refugium for human populations in the Pleistocene. *Quat. Sci. Rev.* **2008**, *27*, 2095–2099. [[CrossRef](#)]
25. Ermolli, E.R.; di Pasquale, G. Vegetation dynamics of south-western Italy in the last 28 kyr inferred from pollen analysis of a Tyrrhenian Sea core. *Veg. Hist. Archaeobot.* **2002**, *11*, 211–220. [[CrossRef](#)]
26. Svenning, J.-C.; Normand, S.; Kageyama, M. Glacial refugia of temperate trees in Europe: Insights from species distribution modelling. *J. Ecol.* **2008**, *96*, 1117–1127. [[CrossRef](#)]
27. Spada, F.; Cutini, M.; Paura, B. Floristic changes along the topographical gradient in montane grasslands in Monti Picentini (Campania, SW Italy). *Ann. Bot.* **2010**, *0*, 86–98.
28. Bucci, G.; Borghetti, M. Understory vegetation as a useful predictor of natural regeneration and canopy dynamics in *Pinus sylvestris* forests in Italy. *Acta Oecol.* **1997**, *18*, 485–501. [[CrossRef](#)]
29. Santangelo, N.; Santo, A.; Guida, D.; Lanzara, R.; Siervo, V. The geosites of the Cilento-Vallo di Diano National Park (Campania region, southern Italy). *Quat. Vol. Spec.* **2005**, *18*, 104–114.
30. Martini, F. *Grotta della Serratura a Marina di Camerota. Culture e Ambienti dei Complessi Olocenici*; Garlatti & Razzai: Firenze, Italy, 1993.
31. Martini, I.; Ronchitelli, A.; Arrighi, S.; Capecchi, G.; Ricci, S.; Scaramucci, S.; Spagnolo, V.; Gambassini, P.; Moroni, A. Cave clastic sediments as a tool for refining the study of human occupation of prehistoric sites: Insights from the cave site of La Cala (Cilento, southern Italy). *J. Quat. Sci.* **2018**, *33*, 586–596. [[CrossRef](#)]
32. Bonanomi, G.; Rita, A.; Allevato, E.; Cesarano, G.; Saulino, L.; Di Pasquale, G.; Allegrezza, M.; Pesaresi, S.; Borghetti, M.; Rossi, S. Anthropogenic and environmental factors affect the tree line position of *Fagus sylvatica* along the Apennines (Italy). *J. Biogeogr.* **2018**, *45*, 2595–2608. [[CrossRef](#)]
33. Greguss, P. *Identification of Living Gymnosperms on the Basis of Xylotomy*; Akadémiai Kiadó: Budapest, Hungary, 1955.
34. Greguss, P. *Holzanatomie der Europäischen Laubhölzer und Sträucher*; Akadémiai Kiadó: Budapest, Hungary, 1959.
35. Schweingruber, F.H. *Anatomie Europäischer Hölzer: Ein Atlas zur Bestimmung Europäischer Baum-, Strauch- und Zwergstrauchhölzer*; P. Haupt: Bern, Switzerland; Stuttgart, Germany, 1990.
36. Vernet, J.L.; Ogereau, P.; Figueiral, I.; Machado Yanes, C.; Uzquiano, P. *Guide D'identification des Charbons de Bois Préhistoriques du Sud-Ouest de l'Europe*; CNRS: Paris, France, 2001.
37. Cambini, A. *Micrografia Comparata dei Legni del Genere Quercus*; Riconoscimento Microscopico del Legno delle Querce Italiane; CNR: Rome, Italy, 1967.
38. Chabal, L.; Fabre, J.F.; Terral, I.; Théry-Parisot, I. L'anthracologie. In *La Botanique*; Bourquin-Mignot, C., Brochier, J.E., Chabal, L., Crozat, S., Fabre, L., Guibal, F., Marival, P., Terral, J.F., Théry-Parisot, I., Eds.; Errance: Paris, France, 1999; pp. 43–104.
39. Chabal, L. La représentativité paléo-écologique des charbons de bois archéologiques issus du bois de feu. *Bull. Soc. Bot. Fr. Actual. Bot.* **1992**, *139*, 213–236. [[CrossRef](#)]
40. Heinz, C.; Thiébaud, S. Characterization and paleoecological significance of archaeological charcoal assemblages during late and post-glacial phases in southern France. *Quat. Res.* **1998**, *50*, 56–68. [[CrossRef](#)]
41. Asouti, E.; Austin, P. Reconstructing woodland vegetation and its exploitation by past societies, based on the analysis and interpretation of archaeological wood charcoal macro-remains. *Environ. Archaeol.* **2005**, *10*, 1–18. [[CrossRef](#)]
42. Di Pasquale, G.; Allevato, E.; Cocchiara, A.; Moser, D.; Pacciarelli, M.; Saracino, A. Late Holocene persistence of *Abies alba* in low-mid altitude deciduous forests of central and southern Italy: New perspectives from charcoal data. *J. Veg. Sci.* **2014**, *25*, 1299–1310. [[CrossRef](#)]
43. Caudullo, G.; Welk, E.; San-Miguel-Ayanz, J. Chorological maps for the main European woody species. *Data Brief* **2017**, *12*, 662–666. [[CrossRef](#)] [[PubMed](#)]
44. Ancillotto, L.; Mori, E.; Bosso, L.; Agnelli, P.; Russo, D. The Balkan long-eared bat (*Plecotus kolombatovici*) occurs in Italy—first confirmed record and potential distribution. *Mamm. Biol.* **2019**, *96*, 61–67. [[CrossRef](#)]

45. Shiferaw, H.; Schaffner, U.; Bewket, W.; Alamirew, T.; Zeleke, G.; Teketay, D.; Eckert, S. Modelling the current fractional cover of an invasive alien plant and drivers of its invasion in a dryland ecosystem. *Sci. Rep.* **2019**, *9*, 1–12. [[CrossRef](#)] [[PubMed](#)]
46. Brown, J.L.; Bennett, J.R.; French, C.M. ENMtoolbox 2.0: The next generation Python-based GIS toolkit for landscape genetic, biogeographic and species distribution model analyses. *PeerJ* **2017**, *5*, e4095. [[CrossRef](#)] [[PubMed](#)]
47. Bosso, L.; Ancillotto, L.; Smeraldo, S.; D'Arco, S.; Migliozi, A.; Conti, P.; Russo, D. Loss of potential bat habitat following a severe wildfire: A model-based rapid assessment. *Int. J. Wildland Fire* **2018**, *27*, 756–769. [[CrossRef](#)]
48. Abdelaal, M.; Fois, M.; Fenu, G.; Bacchetta, G. Using MaxEnt modeling to predict the potential distribution of the endemic plant *Rosa arabica* Crép. in Egypt. *Ecol. Inform.* **2019**, *50*, 68–75. [[CrossRef](#)]
49. Smeraldo, S.; Bosso, L.; Fraissinet, M.; Bordignon, L.; Brunelli, M.; Ancillotto, L.; Russo, D. Modelling risks posed by wind turbines and power lines to soaring birds: The black stork (*Ciconia nigra*) in Italy as a case study. *Biodivers. Conserv.* **2020**, *29*, 1–18. [[CrossRef](#)]
50. Phillips, S.J.; Anderson, R.P.; Dudík, M.; Schapire, R.E.; Blair, M.E. Opening the black box: An open-source release of Maxent. *Ecography* **2017**, *40*, 887–893. [[CrossRef](#)]
51. Raffini, F.; Bertorelle, G.; Biello, R.; D'Urso, G.; Russo, D.; Bosso, L. From Nucleotides to Satellite Imagery: Approaches to Identify and Manage the Invasive Pathogen *Xylella fastidiosa* and Its Insect Vectors in Europe. *Sustainability* **2020**, *12*, 4508. [[CrossRef](#)]
52. Bertolino, S.; Sciandra, C.; Bosso, L.; Russo, D.; Lurz, P.W.; Di Febbraro, M. Spatially explicit models as tools for implementing effective management strategies for invasive alien mammals. *Mammal Rev.* **2020**, *50*, 187–199. [[CrossRef](#)]
53. Iverson, L.R.; Rebeck, J.; Peters, M.P.; Hutchinson, T.; Fox, T. Predicting *Ailanthus altissima* presence across a managed forest landscape in southeast Ohio. *For. Ecosyst.* **2019**, *6*, 1–13. [[CrossRef](#)]
54. Sillero, N.; Poboljšaj, K.; Lešnik, A.; Šalamun, A. Influence of landscape factors on amphibian roadkills at the national level. *Diversity* **2019**, *11*, 13. [[CrossRef](#)]
55. Zarzo-Arias, A.; Penteriani, V.; del Mar Delgado, M.; Torre, P.P.; Garcia-Gonzalez, R.; Mateo-Sánchez, M.C.; Garcia, P.V.; Dalerum, F. Identifying potential areas of expansion for the endangered brown bear (*Ursus arctos*) population in the Cantabrian Mountains (NW Spain). *PLoS ONE* **2019**, *14*, e0209972. [[CrossRef](#)] [[PubMed](#)]
56. Fois, M.; Bacchetta, G.; Cuenca-Lombrana, A.; Cogoni, D.; Pinna, M.S.; Sulis, E.; Fenu, G. Using extinctions in species distribution models to evaluate and predict threats: A contribution to plant conservation planning on the island of Sardinia. *Environ. Conserv.* **2018**, *45*, 11–19. [[CrossRef](#)]
57. Phillips, S.J.; Dudík, M. Modeling of species distributions with Maxent: New extensions and a comprehensive evaluation. *Ecography* **2008**, *31*, 161–175. [[CrossRef](#)]
58. Wang, R.; Li, Q.; He, S.; Liu, Y.; Wang, M.; Jiang, G. Modeling and mapping the current and future distribution of *Pseudomonas syringae* pv. *actinidiae* under climate change in China. *PLoS ONE* **2018**, *13*, e0192153.
59. Merow, C.; Smith, M.J.; Silander, J.A. A practical guide to MaxEnt for modeling species' distributions: What it does, and why inputs and settings matter. *Ecography* **2013**, *36*, 1058–1069. [[CrossRef](#)]
60. Leipold, M.; Tausch, S.; Poschlod, P.; Reisch, C. Species distribution modeling and molecular markers suggest longitudinal range shifts and cryptic northern refugia of the typical calcareous grassland species *Hippocrepis comosa* (horseshoe vetch). *Ecol. Evol.* **2017**, *7*, 1919–1935. [[CrossRef](#)]
61. Roces-Díaz, J.V.; Jiménez-Alfaro, B.; Chytrý, M.; Díaz-Varela, E.R.; Álvarez-Álvarez, P. Glacial refugia and mid-Holocene expansion delineate the current distribution of *Castanea sativa* in Europe. *Paleogeogr. Paleoclimatol. Paleoecol.* **2018**, *491*, 152–160. [[CrossRef](#)]
62. Dakhil, M.A.; Xiong, Q.; Farahat, E.A.; Zhang, L.; Pan, K.; Pandey, B.; Olatunji, O.A.; Tariq, A.; Wu, X.; Zhang, A. Past and future climatic indicators for distribution patterns and conservation planning of temperate coniferous forests in southwestern China. *Ecol. Indic.* **2019**, *107*, 105559. [[CrossRef](#)]
63. Paz, A.; González, A.; Crawford, A.J. Testing effects of Pleistocene climate change on the altitudinal and horizontal distributions of frogs from the Colombian Andes: A species distribution modeling approach. *Front. Biogeogr.* **2019**, *11*, e37055. [[CrossRef](#)]
64. Archis, J.N.; Akcali, C.; Stuart, B.L.; Kikuchi, D.; Chunco, A.J. Is the future already here? The impact of climate change on the distribution of the eastern coral snake (*Micrurus fulvius*). *PeerJ* **2018**, *6*, e4647. [[CrossRef](#)]

65. Jarnevich, C.S.; Hayes, M.A.; Fitzgerald, L.A.; Adams, A.A.Y.; Falk, B.G.; Collier, M.A.; Lea’R, B.; Klug, P.E.; Naretto, S.; Reed, R.N. Modeling the distributions of tegu lizards in native and potential invasive ranges. *Sci. Rep.* **2018**, *8*, 10193. [[CrossRef](#)] [[PubMed](#)]
66. Fielding, A.H.; Bell, J.F. A review of methods for the assessment of prediction errors in conservation presence/absence models. *Environ. Conserv.* **1997**, *24*, 38–49. [[CrossRef](#)]
67. Warren, D.L.; Seifert, S.N. Ecological niche modeling in Maxent: The importance of model complexity and the performance of model selection criteria. *Ecol. Appl.* **2011**, *21*, 335–342. [[CrossRef](#)] [[PubMed](#)]
68. Elith, J.; Kearney, M.S.; Phillips, S.J. The art of modelling range-shifting species. *Methods Ecol. Evol.* **2010**, *1*, 330–342. [[CrossRef](#)]
69. Pignatti, S. *Flora d’Italia*; Edagricole: Bologna, Italy, 1982.
70. Stoklosa, J.; Daly, C.; Foster, S.D.; Ashcroft, M.B.; Warton, D.I. A climate of uncertainty: Accounting for error in climate variables for species distribution models. *Methods Ecol. Evol.* **2015**, *6*, 412–423. [[CrossRef](#)]
71. Costa, M.; Morla, C.; Sainz Ollero, H. *Los Bosques Ibéricos: Una Interpretación Geobotánica*; Iberian Forests: A Geobotanical Interpretation; Planeta: Madrid, Spain, 1997.
72. Tutin, T.G.; Heywood, V.H.; Burges, N.A.; Valentine, D.H.; Walters, S.M.; Webb, D.A. *Flora Europaea Vol. 1*; Cambridge University Press: Cambridge, UK, 1964.
73. Bernetti, G. *Selvicoltura Speciale*; Unione Tipografico-Editrice Torinese: Torino, Italy, 1995.
74. Finlayson, G.; Finlayson, C.; Pacheco, F.G.; Vidal, J.R.; Carrión, J.S.; Espejo, J.R. Caves as archives of ecological and climatic changes in the Pleistocene—The case of Gorham’s Cave, Gibraltar. *Quat. Int.* **2008**, *181*, 55–63. [[CrossRef](#)]
75. Lambeck, K.; Purcell, A. Sea-level change in the Mediterranean Sea since the LGM: Model predictions for tectonically stable areas. *Quat. Sci. Rev.* **2005**, *24*, 1969–1988. [[CrossRef](#)]
76. Di Donato, V.; Esposito, P.; Russo-Ermolli, E.; Scarano, A.; Cheddadi, R. Coupled atmospheric and marine paleoclimatic reconstruction for the last 35 ka in the Sele Plain–Gulf of Salerno area (southern Italy). *Quat. Int.* **2008**, *190*, 146–157. [[CrossRef](#)]
77. Mix, A.C.; Bard, E.; Schneider, R. Environmental processes of the ice age: Land, oceans, glaciers (EPILOG). *Quat. Sci. Rev.* **2001**, *20*, 627–657. [[CrossRef](#)]
78. Tzedakis, P.C. Seven ambiguities in the Mediterranean paleoenvironmental narrative. *Quat. Sci. Rev.* **2007**, *26*, 2042–2066. [[CrossRef](#)]
79. Allen, J.R.; Huntley, B. Weichselian palynological records from southern Europe: Correlation and chronology. *Quat. Int.* **2000**, *73*, 111–125. [[CrossRef](#)]
80. Ellenberg, H. *Zeigerwerte der Gefäßpflanzen Mitteleuropas*; Scripta Geobotanica IX; Erich Goltze KG: Göttingen, Germany, 1979.
81. Bertolini, M.; Fedozzi, S.; Martini, F.; Sala, B. Late Glacial and Holocene climatic oscillations inferred from the variations in the micromammal associations at Grotta della Serratura (Marina di Camerota, Salerno, S. Italy). *Quaternario* **1996**, *9*, 561–566.
82. Sala, B. Climatic changes in the Quaternary inferred from variations in the Mammal associations. *Allionia* **1996**, *9*, 89–94.
83. Martini, F.; Colonese, A.C.; Giuseppe, Z.D.; Ghinassi, M.; Vetro, D.L.; Ricciardi, S. Human-environment relationships during the Late Glacial-Early Holocene transition: Some examples from Campania, Calabria and Sicily. *Méditerranée* **2009**, *112*, 89–94. [[CrossRef](#)]
84. Follieri, M.; Giardini, M.; Magri, D.; Sadori, L. Palynostratigraphy of the last glacial period in the volcanic region of central Italy. *Quat. Int.* **1998**, *47*, 3–20. [[CrossRef](#)]
85. Magri, D. Advances in Italian palynological studies: Late Pleistocene and Holocene records. *GFF* **2007**, *129*, 337–344. [[CrossRef](#)]
86. Ricci Lucchi, M.R. Vegetation dynamics during the last Interglacial–Glacial cycle in the Arno coastal plain (Tuscany, western Italy): Location of a new tree refuge. *Quat. Sci. Rev.* **2008**, *27*, 2456–2466. [[CrossRef](#)]
87. Fiorentino, G. L’analisi antracologica della sepoltura Ostuni 1 di S. Maria di Agnano: Considerazioni paleoambientali e paleontologiche. In *Il Riparo di Agnano nel Paleolitico Superiore: La Sepoltura Ostuni 1 e Suoi Simboli*; Coppola, D., Ed.; Università di Roma Tor Vergata: Rome, Italy, 2012; pp. 197–201.
88. García-Amorena, I.; Manzanque, F.G.; Rubiales, J.M.; Granja, H.M.; de Carvalho, G.S.; Morla, C. The Late Quaternary coastal forests of western Iberia: A study of their macroremains. *Paleogeogr. Paleoclimatol. Paleoecol.* **2007**, *254*, 448–461. [[CrossRef](#)]

89. Hallé, F.; Oldemann, R.A.A.; Tomlinson, P.B. *Tropical Trees and Forests: An Architectural Analysis*; Springer: Berlin, Germany, 1978.
90. Farjon, A. *Pines: Drawings and Description of the Genus Pinus*, 2nd ed.; Brill Academic Pub: Leiden, The Netherlands, 2018.
91. Todaro, L.; Andreu, L.; D'Alessandro, C.M.; Gutiérrez, E.; Cherubini, P.; Saracino, A. Response of *Pinus leucodermis* to climate and anthropogenic activity in the National Park of Pollino (Basilicata, Southern Italy). *Biol. Conserv.* **2007**, *137*, 507–519. [[CrossRef](#)]
92. Quézel, P.; Barbero, M. Signification phytoécologique et phytosociologique des peuplements naturels de Pin de Salzmann en France. *Ecol. Mediterr.* **1988**, *14*, 41–63. [[CrossRef](#)]
93. Akman, Y. The vegetation of Beynam forest. *Commun. Fac. Sci. Univ. Ank.* **1972**, *16*, 31–54. [[CrossRef](#)]
94. Emberger, L. La végétation de la région méditerranéenne. Essai d'une classification des groupements végétaux. *Rev. Gen. Bot.* **1930**, *503*, 642–662.
95. Orombelli, G.; Ravazzi, C.; Cita, M.B. Osservazioni sul significato dei termini LGM (UMG), Tardoglaciale e postglaciale in ambito globale, italiano ed alpino. *Quaternario* **2005**, *18*, 147–156.
96. Watts, W.A.; Allen, J.R.M.; Huntley, B.; Fritz, S.C. Vegetation history and climate of the last 15,000 years at Laghi di Monticchio, southern Italy. *Quat. Sci. Rev.* **1996**, *15*, 113–132. [[CrossRef](#)]
97. Follieri, M.; Magri, D.; Sadori, L. 250,000-year pollen record from Valle di Castiglione (Roma). *Pollen Spores* **1988**, *30*, 329–356.
98. Kelly, M.G.; Huntley, B. An 11 000-year record of vegetation and environment from Lago di Martignano, Latium, Italy. *J. Quat. Sci.* **1991**, *6*, 209–224. [[CrossRef](#)]
99. Leroy, S.A.G.; Giralt, S.; Francus, P.; Seret, G. The high sensitivity of the palynological record in the Vico maar lacustrine sequence (Latium, Italy) highlights the climatic gradient through Europe for the last 90 ka. *Quat. Sci. Rev.* **1996**, *15*, 189–201. [[CrossRef](#)]
100. Magri, D.; Sadori, L. Late Pleistocene and Holocene pollen stratigraphy at Lago di Vico, central Italy. *Veg. Hist. Archaeobot.* **1999**, *8*, 247–260. [[CrossRef](#)]
101. Magri, D. Late Quaternary vegetation history at Lagaccione near Lago di Bolsena (central Italy). *Rev. Paleobot. Palynol.* **1999**, *106*, 171–208. [[CrossRef](#)]
102. Nicol-Pichard, S.; Dubar, M. Reconstruction of late-glacial and holocene environments in southeast France based on the study of a 66-m long core from Biot, Alpes Maritimes. *Veg. Hist. Archaeobot.* **1998**, *7*, 11–15. [[CrossRef](#)]
103. Colonese, A.C.; Zanchetta, G.; Fallick, A.E.; Martini, F.; Manganelli, G.; Drysdale, R.N. Stable isotope composition of *Helix ligata* (Müller, 1774) from Late Pleistocene–Holocene archaeological record from Grotta della Serratura (Southern Italy): Paleoclimatic implications. *Glob. Planet. Chang.* **2010**, *71*, 249–257. [[CrossRef](#)]
104. Rubiales, J.M.; García-Amorena, I.; Hernández, L.; Génova, M.; Martínez, F.; Manzanque, F.G.; Morla, C. Late Quaternary dynamics of pinewoods in the Iberian mountains. *Rev. Paleobot. Palynol.* **2010**, *162*, 476–491. [[CrossRef](#)]
105. Carrión, J.S.; Finlayson, C.; Fernández, S.; Finlayson, G.; Allué, E.; López-Sáez, J.A.; López-García, P.; Gil-Romera, G.; Bailey, G.; González-Sampériz, P. A coastal reservoir of biodiversity for Upper Pleistocene human populations: Paleoecological investigations in Gorham's Cave (Gibraltar) in the context of the Iberian Peninsula. *Quat. Sci. Rev.* **2008**, *27*, 2118–2135. [[CrossRef](#)]
106. Carrión, J.S.; Yll, E.I.; Walker, M.J.; Legaz, A.J.; Chaín, C.; López, A. Glacial refugia of temperate, Mediterranean and Ibero-North African flora in south-eastern Spain: New evidence from cave pollen at two Neanderthal man sites. *Glob. Ecol. Biogeogr.* **2003**, *12*, 119–129. [[CrossRef](#)]
107. Huntley, B.; Birks, H.J.B. *An Atlas of Past and Present Pollen Maps for Europe: 0–13000 Years Ago*; Cambridge University Press: Cambridge, UK, 1983.
108. Tzedakis, P.C. Vegetation change through glacial—Interglacial cycles: A long pollen sequence perspective. *Philos. Trans. R. Soc. Lond. Ser. B Biol. Sci.* **1994**, *345*, 403–432.
109. Willis, K.; Mc Elwain, J. *The Evolution of Plants*; Oxford University Press: Oxford, UK, 2013.

